

## WILDFIRES

## Wildfire smoke destroys stratospheric ozone

Peter Bernath<sup>1,2,3\*</sup>, Chris Boone<sup>2</sup>, Jeff Crouse<sup>2</sup>

Large wildfires inject smoke and biomass-burning products into the mid-latitude stratosphere, where they destroy ozone, which protects us from ultraviolet radiation. The infrared spectrometer on the Atmospheric Chemistry Experiment satellite measured the spectra of smoke particles from the “Black Summer” fires in Australia in late 2019 and early 2020, revealing that they contain oxygenated organic functional groups and water adsorption on the surfaces. These injected smoke particles have produced unexpected and extreme perturbations in stratospheric gases beyond any seen in the previous 15 years of measurements, including increases in formaldehyde, chlorine nitrate, chlorine monoxide, and hypochlorous acid and decreases in ozone, nitrogen dioxide, and hydrochloric acid. These perturbations in stratospheric composition have the potential to affect ozone chemistry in unexpected ways.

The occurrence and severity of wildfires have been increasing as a result of climate change (1). Recently, there have been several extreme wildfires, including the “Black Saturday” bushfires in Australia in 2009 (2), wildfires in the Pacific Northwest of North America in 2017 (3), and more severe “Black Summer” bushfires in Australia in 2019 and 2020 (4). Severe fires can create pyrocumulonimbus clouds (pyroCb) (5) that rapidly transport fire products into the upper troposphere and sometimes even into the lower stratosphere (6). PyroCbs can affect climate by heating the stratosphere and cooling Earth’s surface (7); stratospheric chemistry may also be affected (2), and it is likely that climate change will also increase the occurrence of pyroCbs (8).

Extreme pyroCbs have been compared to moderate volcanic eruptions (9) and “nuclear winter” (4) because of the increase in stratospheric aerosols from smoke. Similar to large volcanic eruptions, pyroCbs can decrease stratospheric ozone (O<sub>3</sub>), which shields us from damaging ultraviolet radiation (10). Atmospheric Chemistry Experiment (ACE) satellite (11) observations point to strong perturbations of stratospheric chemistry by pyroCbs that result in stratospheric ozone depletion at mid-latitudes. The Montreal Protocol on Substances that Deplete the Ozone Layer (12) has been successful in reducing the atmospheric abundances of chlorine- and bromine-containing molecules that destroy stratospheric ozone and are responsible for the Antarctic ozone hole (13, 14). The increasing frequency of major wildfires (1, 8), however, has the potential to delay the recovery of stratospheric ozone, which is currently predicted to return to 1980 levels around 2052–2060 (15).

The main instrument on the ACE satellite is a high-resolution infrared Fourier transform spectrometer (FTS), which has been making solar occultation observations of the atmosphere in a limb geometry since 2004 (11). During sunrise and sunset, the ACE-FTS records a sequence of atmospheric absorption spectra using the Sun as a light source. Note that ACE observations occur at twilight, and

abundances of photochemically active molecules such as ClO and HOCl depend on the time at which the measurements are made. These infrared spectra are then analyzed on the ground (16) to provide altitude profiles of volume mixing ratios (VMRs) and concentrations for more than 44 molecules (17) as well as infrared spectra of aerosols and diffuse clouds. ACE also has a visible imager (at 0.525 μm) and a near-infrared imager (at 1.02 μm), both of which provide atmospheric extinction due to clouds and aerosols.

The ACE-FTS has recorded spectra of the material injected into the stratosphere by pyroCbs during the extreme Australian bushfires in late December 2019 to early January 2020 (6). Spectra of stratospheric smoke particles were obtained by removing absorption features as a result of gaseous molecules; a sample aerosol infrared spectrum is shown in Fig. 1. These characteristic spectra show strong absorption features due to C=O, CH, and OH stretching modes consistent with carboxylic acid [–C(O)OH] groups bound to carbon. There is also evidence of adsorbed water from the hydrogen-bonded OH stretching and librational modes. No features

**Fig. 1.** The aerosol spectrum for tangent height 16.6 km from occultation ss88361, measured 6 January 2020 at latitude 58.8°S. In “ss8836,” “ss” stands for sunset and 88361 is the number of orbits since launch, a unique identifier for the measurement. Spectral features associated with selected functional groups are indicated.

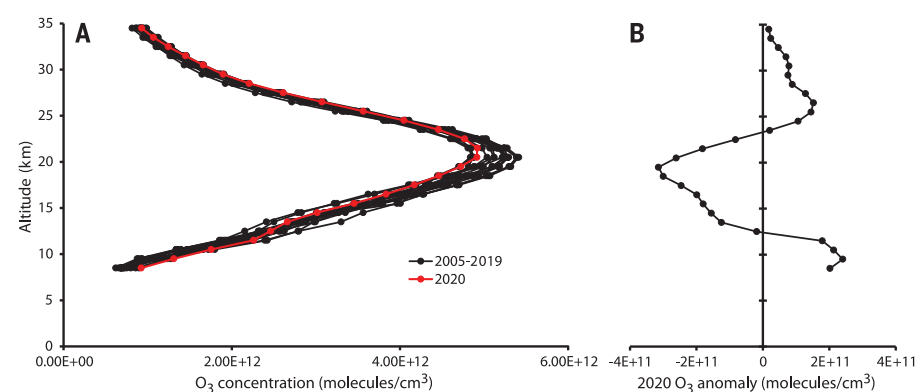
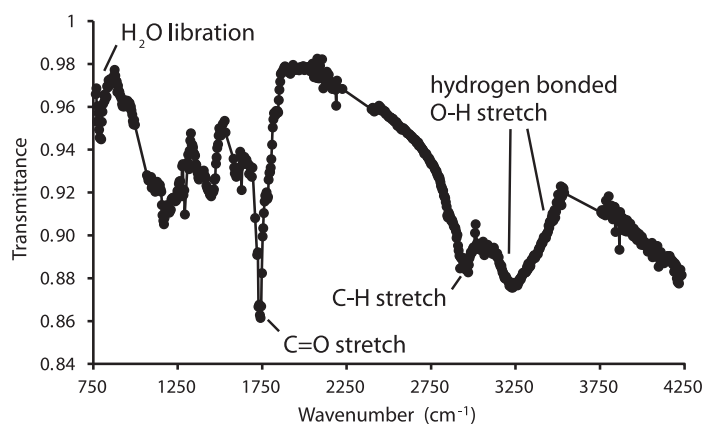


**Fig. 2.** ACE-FTS ozone concentration profiles. (A) The average O<sub>3</sub> concentration profiles for the latitude range 45° to 60°S for ACE-FTS occultations in July. The profiles for all years before 2020 measured by the ACE-FTS are shown in black and the average profile for 2020 is shown in red. (B) The anomaly profile for 2020 O<sub>3</sub> concentration is the 2020 profile in (A) minus the average profile from all other years.

<sup>1</sup>Department of Chemistry and Biochemistry, Old Dominion University, Norfolk, VA, USA. <sup>2</sup>Department of Chemistry, University of Waterloo, Waterloo, ON, Canada. <sup>3</sup>Department of Physics, Old Dominion University, Norfolk, VA, USA. \*Corresponding author. Email: pbernath@odu.edu

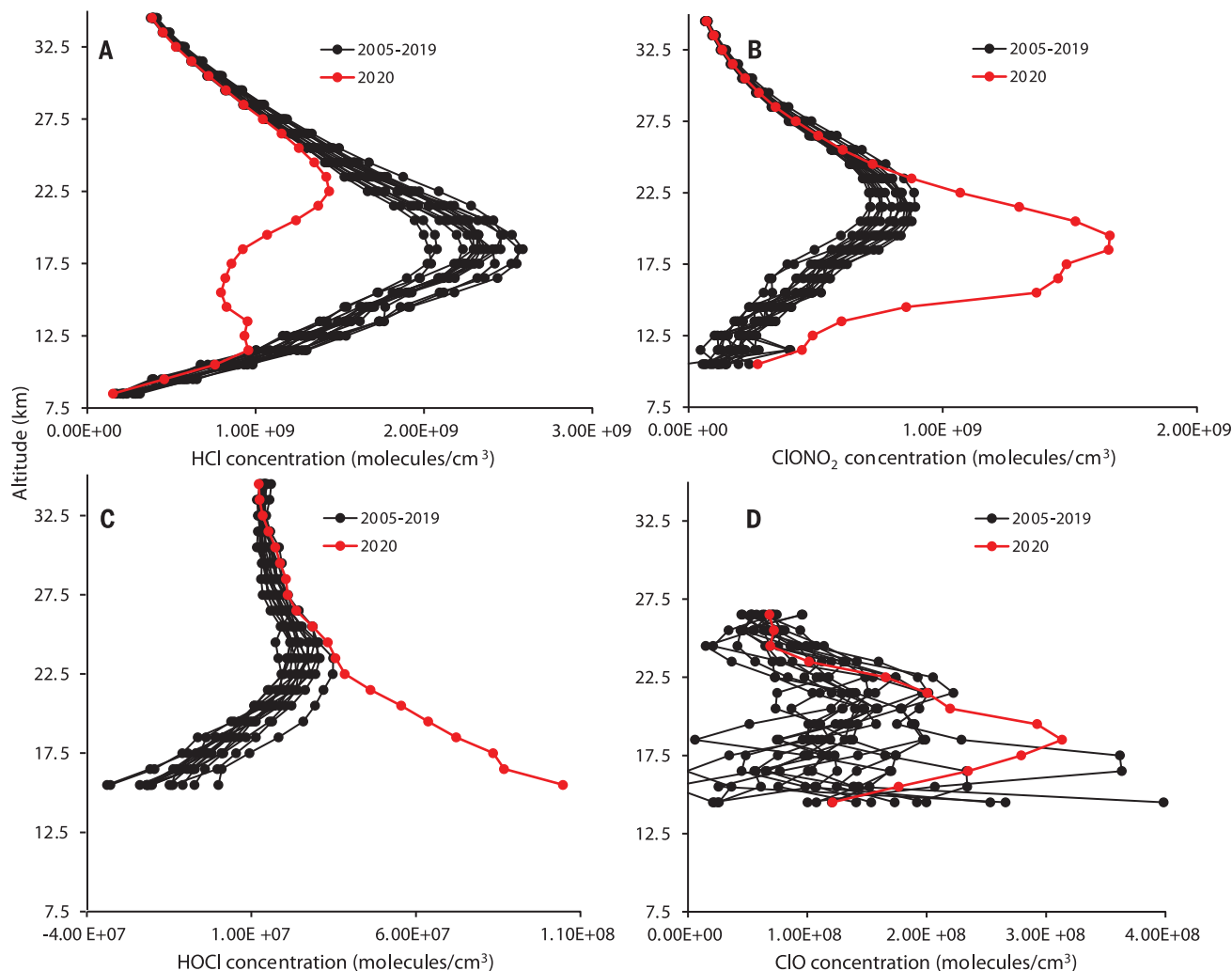


**Fig. 3. Concentrations of chlorine-containing molecules for the latitude range 45° to 60°S for ACE-FTS occultations in late May and early June.** Profiles for all years before 2020 measured by the ACE-FTS are shown in black and the average profile for 2020 is in red. (A) HCl. (B) ClONO<sub>2</sub>. (C) HOCl. (D) ClO.

are assignable to adsorbed sulfuric acid (7). Surface reactions on this acidic, hydrated soot have not yet been studied in the laboratory and are hence unknown. However, here we describe how they are capable of perturbing several species expected to influence ozone, such as nitrogen dioxide and hypochlorous acid. ACE observed enhanced aerosols with the ACE imagers in the Southern Hemisphere stratosphere from January to November 2020, primarily because of the fires (fig. S1).

Average ACE ozone concentrations at mid-latitudes (45° to 60°S) were found to increase in the 8- to 20-km range in January and March 2020 (fig. S2) compared with the average of all other years observed by ACE because of the injection of many organic molecules into the upper troposphere and lower stratosphere. The usual tropospheric oxidation chemistry responsible for ozone pollution (18) is therefore the cause of this early ozone increase af-

ter the pyroCb events. The lifetime of these organic molecules is relatively short, so this enhancement does not persist much beyond March 2020. Starting in April 2020, mid-latitude ozone levels began to decline in the lower stratosphere compared with the average of all other years and remained low through to December 2020 (fig. S3). Fig. 2 shows the ozone profile for July 2020 for 45° to 60°S compared with the average of all other years. Similar ozone declines were observed from 30° to 45°S in the 16- to 26-km altitude range, but no significant declines were observed (5 to 35 km) over Antarctica (prior to Southern Hemisphere winter) or the tropics compared with previous years.

Some years had O<sub>3</sub> levels near 18 km during certain months that were lower or comparable to those observed in 2020: for example, 2005 and 2008 in July (Fig. 2), 2008 in May and June, and 2006 in October (fig. S3). However, no other year exhibited persistently

low O<sub>3</sub> levels (compared with other years measured by ACE) over such an extended period of time. Later in the year (October and December; fig. S3), average O<sub>3</sub> near 18 km for 2020 in this latitude range was well below the typical range of variability established by measurements from previous years.

The stratospheric chemistry of ozone is well known to involve HO<sub>x</sub> radicals (H, OH, and HO<sub>2</sub>), halogen chemistry (Cl and Br), and reactive nitrogen species (18, 19). Trace gases and soot from pyroCbs perturb each of these reaction families.

Unexpected and notable changes were observed in a range of lower stratospheric, chlorine-containing species from March to August 2020 at 45° to 60°S. ACE-FTS mid-latitude observations show a decrease in hydrochloric acid (HCl) abundance but increases in chlorine nitrate (ClONO<sub>2</sub>), hypochlorous acid (HOCl), and chlorine monoxide (ClO).

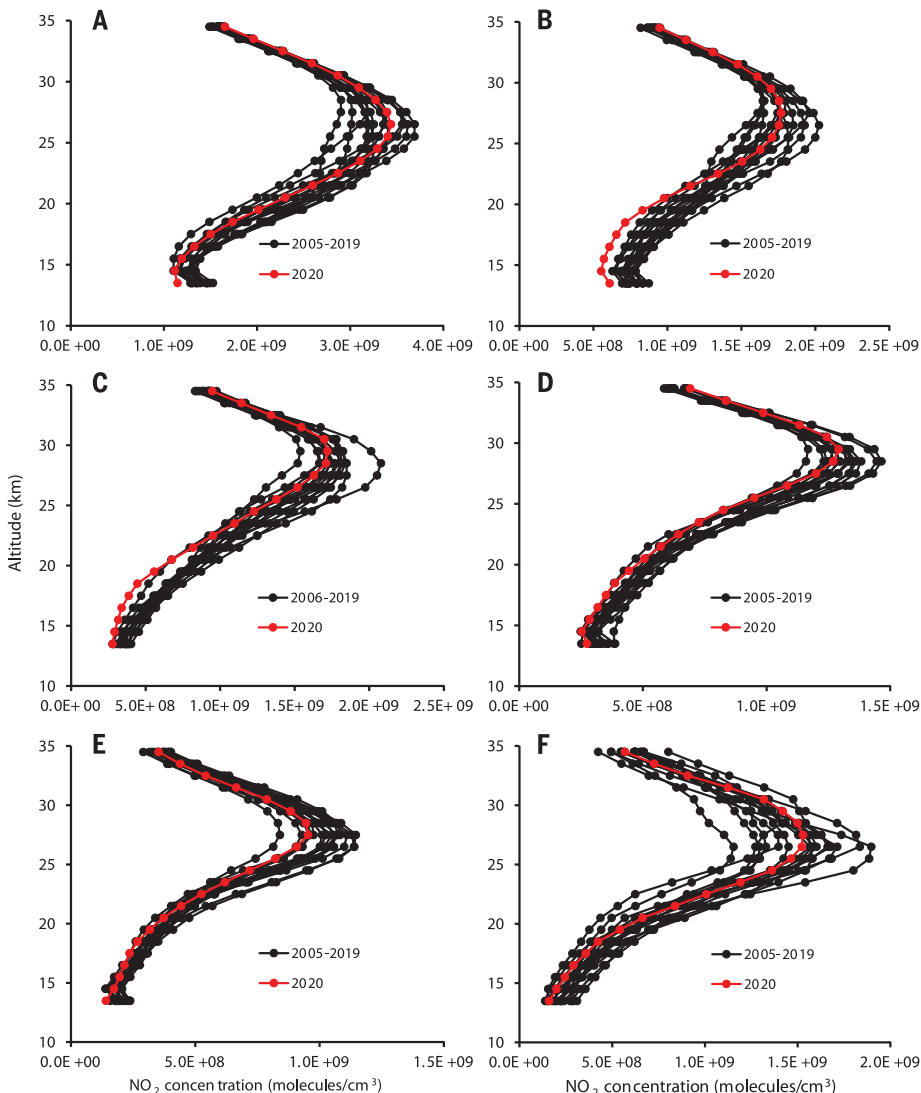


**Fig. 4.**  $\text{NO}_2$  concentration profiles for ACE-FTS measurements in the latitude range  $45^\circ$  to  $60^\circ\text{S}$ .

Average profiles for all years before 2020 are shown in black and the average profile for 2020 is in red. (A) January. (B) March. (C) April. (D) Late May and early June. (E) July. (F) August.

The strong enhancement of HOCl concentrations is particularly notable. HOCl is produced from ClO and ClONO<sub>2</sub>. At mid-latitudes the reaction making HOCl (20, 21) is



The injection of organic molecules into the stratosphere leads to the formation of formaldehyde ( $\text{H}_2\text{CO}$ ) and other sources of  $\text{HO}_2$  radicals (18);  $\text{H}_2\text{CO}$  near 18 km was observed to be enhanced well into 2021 (fig. S4). Photolysis of  $\text{H}_2\text{CO}$  or reaction with hydroxyl radical (OH) leads to the formyl radical (HCO), which reacts with  $\text{O}_2$  to make excess hydroperoxyl radical ( $\text{HO}_2$ ).  $\text{HO}_2$  depletes  $\text{O}_3$  in the  $\text{HO}_x$  cycle ( $\text{OH} + \text{O}_3 \rightarrow \text{HO}_2 + \text{O}_2$ ,  $\text{HO}_2 + \text{O}_3 \rightarrow \text{OH} + 2\text{O}_2$ ) and forms HOCl in reaction 1. HOCl also depletes ozone when it is photolyzed to make OH and Cl, both of which destroy  $\text{O}_3$

in the  $\text{HO}_x$  and  $\text{ClO}_x$  ( $\text{Cl} + \text{O}_3 \rightarrow \text{ClO} + \text{O}_2$ ,  $\text{ClO} + \text{O} \rightarrow \text{Cl} + \text{O}_2$ ) cycles (19).

HOCl production (Fig. 3) from ClONO<sub>2</sub> is also likely catalyzed by hydrated smoke particles,



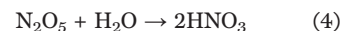
Heterogeneous chemistry of HOCl on smoke then can contribute to the observed reduction (Fig. 3) in HCl abundance through the reaction



The heterogeneous reaction of ClONO<sub>2</sub>+HCl also yields  $\text{Cl}_2$  and is likely to contribute to the loss of HCl.  $\text{Cl}_2$  is photolyzed to Cl atoms, and ozone destruction occurs through the  $\text{ClO}_x$  cycle. Reactions 2 and 3 are known to be catalyzed by polar stratospheric clouds (PSCs)

during Antarctic and Arctic ozone depletion events (18). Similar chemistry can be expected on hydrated acidic smoke particles. The 2020 time series for ClONO<sub>2</sub>, HCl, HOCl, and ClO concentration profiles are presented in figs. S5, S6, S7, and S8, respectively.

Nitrogen dioxide ( $\text{NO}_2$ ) abundances (Fig. 4) were reduced in the 15- to 25-km range at mid-latitudes from January to July 2020 (particularly in March and April). Dinitrogen pentoxide ( $\text{N}_2\text{O}_5$ ) forms at night from  $\text{NO}_2$  and reacts with  $\text{H}_2\text{O}$  in aerosol particles (22),



This reaction is slow in the gas phase but may be catalyzed by hydrated smoke particles analogous to volcanic sulfate aerosol chemistry (23). Galib and Limmer (24) have recently shown that the uptake of  $\text{N}_2\text{O}_5$  on aqueous aerosols is a surface process, supporting the idea that  $\text{N}_2\text{O}_5$  reacts on the hydrated surface of smoke particles. The variability of the  $\text{NO}_2$  profiles in other years is likely a result of stratospheric dynamics (Fig. 4).

ClONO<sub>2</sub> is produced by three-body recombination of ClO and  $\text{NO}_2$  (19). The observed enhancement (Fig. 3) of ClONO<sub>2</sub> means that the increased production of the reactive ClO radical (modest enhancements are observed by ACE-FTS; Fig. 3) offsets the decline in  $\text{NO}_2$ . The perturbation of HCl by smoke is less extreme than that caused by polar stratospheric clouds (PSCs) during polar winter, when HCl abundances can approach zero (19). The observed stratospheric temperatures from ACE-FTS at mid-latitudes are never low enough to produce PSCs. Indeed, the average temperature profiles were elevated from January to March 2020 (fig. S9), consistent with stratospheric heating by smoke particles (7). Polar chlorine chemistry strongly reduces the abundances of both HCl and ClONO<sub>2</sub> by reactions on PSCs in contrast to the reduction in HCl and the increase in ClONO<sub>2</sub> associated with smoke particles.

ACE-FTS observations clearly show that pyroCb organics and smoke cause substantial perturbations in chemical species, demonstrating an unanticipated role in stratospheric chemistry. Although the reductions in  $\text{NO}_x$  will increase  $\text{O}_3$  abundances by suppression of the  $\text{NO}_x$  cycle (18) ( $\text{NO} + \text{O}_3 \rightarrow \text{NO}_2 + \text{O}_2$ ,  $\text{NO}_2 + \text{O} \rightarrow \text{NO} + \text{O}_2$ ), this effect is offset by enhanced  $\text{O}_3$  destruction in the  $\text{ClO}_x$  and  $\text{HO}_x$  cycles. As severe wildfires rise in number, they will play an increasingly important role in the global ozone budget.

## REFERENCES AND NOTES

- IPCC, "Climate Change 2021: The Physical Science Basis. Contribution of Working Group I to the Sixth Assessment Report of the Intergovernmental Panel on Climate Change," V. Masson-Delmotte et al., Eds. (Cambridge Univ. Press, 2021); [www.ipcc.ch/report/ar6/wg1/](http://www.ipcc.ch/report/ar6/wg1/)

2. N. Glatthor *et al.*, *Atmos. Chem. Phys.* **13**, 1637–1658 (2013).
3. S. M. Khaykin *et al.*, *Geophys. Res. Lett.* **45**, 1639–1646 (2018).
4. D. A. Peterson *et al.*, *NPJ Clim. Atmos. Sci.* **4**, 38 (2021).
5. M. Fromm *et al.*, *Bull. Am. Meteorol. Soc.* **91**, 1193–1210 (2010).
6. C. D. Boone, P. F. Bernath, M. D. Fromm, *Geophys. Res. Lett.* **47**, e2020GL088442 (2020).
7. P. Yu *et al.*, *Geophys. Res. Lett.* **48**, e2021GL092609 (2021).
8. G. Di Virgilio *et al.*, *Geophys. Res. Lett.* **46**, 8517–8526 (2019).
9. D. A. Peterson *et al.*, *NPJ Clim. Atmos. Sci.* **1**, 30 (2018).
10. S. Solomon *et al.*, *Proc. Natl. Acad. Sci. U.S.A.* **119**, e2117325119 (2022).
11. P. F. Bernath, *J. Quant. Spectrosc. Radiat. Transf.* **186**, 3–16 (2017).
12. UN Environment Programme, “Montreal protocol on substances that deplete the ozone layer” (1987); <https://ozone.unep.org/treaties/montreal-protocol>.
13. World Meteorological Organization, “Scientific Assessment of Ozone Depletion: 2018. Global Ozone Research and Monitoring Project” (Report No. 58, pp. 588, 2018); <https://csl.noaa.gov/assessments/ozone/2018/>.
14. P. Bernath, A. M. Fernando, *J. Quant. Spectrosc. Radiat. Transf.* **217**, 126–129 (2018).
15. M. Amos *et al.*, *Atmos. Chem. Phys.* **20**, 9961–9977 (2020).
16. C. D. Boone, P. F. Bernath, D. Cok, J. Steffen, S. C. Jones, *J. Quant. Spectrosc. Radiat. Transf.* **247**, 106939 (2020).
17. P. F. Bernath, J. Steffen, J. Crouse, C. D. Boone, *J. Quant. Spectrosc. Radiat. Transf.* **253**, 107178 (2020).
18. B. J. Finlayson-Pitts, J. N. Pitts Jr., *Chemistry of the Upper and Lower Atmosphere: Theory, Experiments, and Applications* (Academic Press, 1980).
19. S. Solomon, *Rev. Geophys.* **37**, 275–316 (1999).
20. T. von Clarmann *et al.*, *Atmos. Chem. Phys.* **12**, 1965–1977 (2012).
21. P. F. Bernath, R. Dodandodage, C. D. Boone, J. Crouse, *J. Quant. Spectrosc. Radiat. Transf.* **264**, 107559 (2021).
22. T. H. Bertram, J. A. Thornton, *Atmos. Chem. Phys.* **9**, 8351–8363 (2009).
23. M. Prather, *J. Geophys. Res.* **97**, 10,187–10,191 (1992).
24. M. Galib, D. T. Limmer, *Science* **371**, 921–925 (2021).

#### ACKNOWLEDGMENTS

P.B. acknowledges R.F. Bernath for productive discussion. **Funding:** Canadian Space Agency contract 9F045-200575/001/SA (P.B.,

C.B., and J.C.) **Author contributions:** Conceptualization: P.B. and C.B. Methodology: C.B. and P.B. Visualization: C.B. and J.C. Funding acquisition: P.B. Supervision: P.B. Writing – original draft: P.B. Writing – review and editing: P.B., C.B., and J.C. **Competing interests:** Authors declare that they have no competing interests. **Data and materials availability:** Data for Fig. 1 are available in the supplementary materials. ACE data, including the HOCl research product, are freely available after sign-up at <https://database.scisat.ca/12signup.php>.

#### SUPPLEMENTARY MATERIALS

[science.org/doi/10.1126/science.abm5611](https://science.org/doi/10.1126/science.abm5611)  
Materials and Methods  
Figs. S1 to S9  
Reference (25)  
Data for Fig. 1

25 September 2021; accepted 11 February 2022  
[10.1126/science.abm5611](https://doi.org/10.1126/science.abm5611)

## Wildfire smoke destroys stratospheric ozone

Peter BernathChris BooneJeff Crouse

*Science*, 375 (6586), • DOI: 10.1126/science.abm5611

### Fired up

Large wildfires can produce ascending atmospheric plumes of such great intensity that they inject smoke and other combustion products into the stratosphere. Bernath *et al.* show that compounds transported into the stratosphere by the Black Summer Australian fires in 2019–2020 caused extreme perturbations in stratospheric gas composition that have the potential to destroy ozone. As climate change causes severe wildfires to become more frequent, their effects on the global ozone budget will grow. —HJS

### View the article online

<https://www.science.org/doi/10.1126/science.abm5611>

### Permissions

<https://www.science.org/help/reprints-and-permissions>